Heliyon 6 (2020) e04496

Contents lists available at ScienceDirect

Heliyon

journal homepage: www.cell.com/heliyon

Research article

Multitemporal optical and radar metrics for wetland mapping at national level in Albania

Javier Muro [a,*], Ana Varea [a], Adrian Strauch [a], Anis Guelmami [b], Eleni Fitoka [c], Frank Thonfeld [f,g], Bernd Diekkrüger [d], Björn Waske [e]

[a] Center for Remote Sensing of Land Surfaces (ZFL), University of Bonn, Bonn, 53113, Germany
[b] Tour du Valat Research Centre for the Conservation of Mediterranean Wetlands, Le Sambuc, 13200, Arles, France
[c] The Greek Biotope/Wetland Centre (EKBY), Greece
[d] Department of Geography, University of Bonn, Bonn, 53113, Germany
[e] Remote Sensing and Digital Image Processing Group at the University of Osnabrück, Osnabrück, 49074, Germany
[f] German Remote Sensing Data Center (DFD), German Aerospace Center (DLR), Münchener Straße 20, 82234, Weßling, Germany
[g] Department of Remote Sensing, University of Würzburg, Oswald-Külpe-Str.86, 97074, Würzburg, Germany

ARTICLE INFO

Keywords:
Environmental science
Geography
Earth sciences
Wetlands
Random forest
Data fusion
Sentinel

ABSTRACT

Wetlands are highly dynamic, with many natural and anthropogenic drivers causing seasonal, periodic or permanent changes in their structure and composition. Thus, it is necessary to use time series of images for accurate classifications and monitoring. We used all available Sentinel-1 and Sentinel-2 images to produce a national wetlands map for Albania. We derived different indices and temporal metrics and investigated their impacts and synergies in terms of mapping accuracy. Best results were achieved when combining Sentinel-1 with Sentinel-2 and its derived indices. We reduced systematic errors and increased the thematic resolution using morphometric characteristics and knowledge-based rules, achieving an overall accuracy of 82%. Results were also validated against field inventories. This methodology can be reproducible to other countries and can be made operational for an integrated planning that considers the food, water, and energy nexus.

1. Introduction

The value of wetlands in terms of ecosystem services is widely recognized by the scientific community (Finlayson et al., 2005; Mitsch and Gosselink, 2000; Russi et al., 2012) and policy makers (e.g. playing important roles in the Paris Agreement, the Sendai Framework for Disaster Risk Reduction, or other multilateral biodiversity related agreements (Ramsar Convention on Wetlands, 2018)). However, wetlands are still being degraded at global scales, and degradation trends have increased since 2000 (Dixon et al., 2016; Ramsar Convention on Wetlands, 2018). The main drivers of these trends are agricultural expansion, intensive wood, sand and gravel harvesting, dam building, agricultural and urban waste, drainage and salinization (Finlayson et al., 2005; Ramsar Convention on Wetlands, 2018). This case study focuses on Albania, a country that hosts one of the few last systems of large and undammed rivers of Europe. Some segments of these rivers are biodiversity hotspots for fish and mollusks and harbor high rates of endemisms (Weiss et al., 2018). However, many other rivers in Albania are heavily dammed. Over 90% of its electricity is already provided by hydropower and authorities are planning to increase investments in it. Besides, another 3000 hydropower projects are planned in the Balkan region (Weiss et al., 2018). Some of these projects have been financed by European public banks (Sikorova and Gallop, 2015), but they are facing strong social opposition from academic, conservation, and local organizations (Sikorova and Gallop, 2015; Vejnovic and Gallop, 2018; Weiss et al., 2018). For instance, 37% of the planned projects are located in protected areas, and opponents argue that there is a lack of disclosure and several negative environmental and social impacts caused by some of these projects (Vejnovic and Gallop, 2018).

According to the Global Outlook on Wetlands (Ramsar Convention on Wetlands, 2018), from the Ramsar Secretariat, properly managed wetlands can directly and indirectly contribute to most of the Sustainable Development Goals (SDGs). This puts wetlands in a central position in the debate about sustainable development. The Ramsar Convention as well as UN Environment are two major stakeholders when it comes to assessing the status and trends of wetland ecosystems and their changes

* Corresponding author.
E-mail address: jmuro@uni-bonn.de (J. Muro).

https://doi.org/10.1016/j.heliyon.2020.e04496
Received 19 July 2019; Received in revised form 3 February 2020; Accepted 15 July 2020

over time. Within the framework of the SDGs, especially indicator 6.6.1 "Change in the extent of water-related ecosystems over time" directly requires countries to report on their national wetlands regularly ("UN stats Metadata repository," 2018). Earth Observation (EO) can generate the information that policy makers need to make and justify decisions, and can also support efficiently the implementation of the SDGs (Paganini et al., 2018). The GEO-Wetlands Initiative is a collaborative partnership aiming to make this step as easy as possible for countries by providing methods, tools, guidelines, training and knowledge [www.geowetlands.org]. This case study is one example of how state-of-the-art EO technology can efficiently support wetland mapping and monitoring at national scale.

The last official inventory of wetlands of Albania is from 2003 and it was part of the MedWet Inventory System initiative (Marieta et al., 2003; Perennou et al., 2012). Since then, the paradigm in EO has experienced a revolution with an increasing number of freely available data sets, fusion of Synthetic Aperture Radar (SAR) and optical sensors, general advances in algorithms for classification and modelling, and ultimately, the cloud computing platforms (Gorelick et al., 2017; Joshi et al., 2016; Stefanski et al., 2014; Waske and Benediktsson, 2007). Mapping large areas that include dynamic cover types such as wetlands, with sufficient thematic resolution and accuracy, requires the use of large numbers of images from different sensors. This poses a challenge in terms of available computing power and on technical capacity, both factors considered as bottlenecks that hinder development and the implementation of informed land management policies and plans of developing countries. Cloud computing platforms offer new opportunities to bypass these bottlenecks and to process large amounts of information on an operational basis. They have prompted a number of studies that use time series of images for classification of either specific land cover types classes (e.g. rice mapping (Dong et al., 2016), open water bodies (Hardy et al., 2019), cropland extent (Xiong et al., 2017) or settlements (Patel et al., 2015)), or more complex land cover maps at national (Mack et al., 2017) or even at continental scale (Pflugmacher et al., 2019). Mapping at national scales is a more practical approach, since monitoring and reporting tasks are often needed at national level. Time series of images can be processed using data fusion techniques (Gevaert and García-Haro, 2015), data interpolation (Inglada et al., 2017) best pixel selection (Griffiths et al., 2013), fitting time series functions (Zhu and Woodcock, 2014), or aggregation of data into meaningful multitemporal metrics (Carrasco et al., 2019; Mack et al., 2017; Mahdianpari et al., 2018; Pflugmacher et al., 2019). These metrics (e.g. maximum, mean and minimum) can be applied to the bands directly or to indices derived from them. They are representative of the different seasonal stages of the land cover caused by phenological, land use, or inundation regimes. Time series of SAR imagery are instrumental in covering the complete seasonality of wetlands (Muro et al., 2019; White et al., 2015), especially in areas of persistent cloud cover where images from the dry period and rainy (and therefore cloudy) period are needed. Using both, SAR and multispectral imagery has proven to achieve higher classification accuracies (Joshi et al., 2016; Stefanski et al., 2014; Waske, 2014).

Even when using the full spectral and temporal resolution, there are limitations to the classification power of EO. Coupling EO data with other spatial information can return higher accuracies and increase the thematic resolution (Manandhar et al., 2009; Stefanov et al., 2001; Van der Voorde et al., 2007; Wilkinson, 1996). Examples of the use of ancillary spatial information in mapping tasks include: topographic information (Hird et al., 2017; Lang et al., 2013), spatial explicit metrics (size, shape, edge length) (Herold et al., 2003), precipitation distribution (Pflugmacher et al., 2019) or distance to water bodies and elevation ranges (Long and Skewes, 1996) among many others.

We use the cloud computing platform Google Earth Engine (GEE), to map the wetlands of Albania at national scale by using the whole archive of Sentinel-1 and Sentinel-2 imagery for the period June 2015–June 2018, and a set of flexible knowledge-based rules.

The purpose of this study is to:

- Assess whether the combination of optical and SAR data with knowledge-based rules enhances the classification of wetlands.
- Apply the methodology and demonstrate how it can help to fulfill reporting commitments at national level.
- Update the inventory of Albanian wetlands for the target year 2017.

2. Materials and methods

2.1. Study area

Albania (Figure 1) has an area of 28.784 km^2. It has a steep orography in the east, with most rivers flowing westwards across extensions of floodplains used for agriculture. Several segments of many rivers have been channelized and there are abundant small dams used to store water and produce hydropower scattered over the country. However, there are still several large rivers that remain in pristine conditions (Weiss et al., 2018). Agriculture, energy and tourism are three of its strongest economic sectors (EcoAlbania, 2017; FAO, 2015).

2.2. Datasets

We used all the Sentinel-1A and Sentinel-2A images available in GEE from June 2015 to June 2018. Sentinel-1 images are provided with dual polarization (VV/VH) and as Ground Range Detected. They have been processed by GEE in the Sentinel Application Platform (SNAP) using the following steps: Apply orbit file, noise removal, thermal noise removal, radiometric calibration, terrain correction using SRTM 30, and conversion to dB via log scaling (GEE, 2018). Sentinel-2 images are processed to top-of-atmosphere values. Thus, we used imagery from around 100 overpasses for Sentinel-2, and 264 overpasses for Sentinel-1. Out of all the Sentinel-2 imagery acquired we created a median composite (dataset S2 henceforth). Clouds were masked using the quality band of the Level-1C products (ESA, 2012), and cloud shadows were masked using azimuth and zenith angles to estimate the position of the shadow. Out of the same Sentinel-2 images we created another multitemporal composite using the 90th and 50th percentiles of three indices; the normalized difference vegetation index (NDVI) (Tucker, 1979) (1), the normalized difference water index (NDWI) (Mc Feeters, 1996) (2), and the normalized difference built-up index (NDBI) (Zha et al., 2003) (3). The 90th and 50th percentiles of these indices represent the maximum and median conditions of vegetation and water. Minimum metrics were not used because they were too affected by cloud and shadow noise, and the maxima of the NDBI already correspond to the minima of NDWI and NDVI. We refer to this dataset as NDIs (normalized difference indices).

$$NDVI = \frac{B8a - B4}{B8a + B4} \quad (1)$$

$$NDWI = \frac{B3 - B8a}{B3 + B8a} \quad (2)$$

$$NDBI = \frac{B11 - B8a}{B11 + B8a} \quad (3)$$

Out of the Sentinel-1A images accessed, we created another multitemporal composite (dataset S1 henceforth) using the 99th, 50th, and 5th percentiles of both polarizations and in ascending orbit. We used the 5th percentile instead of the 1st to eliminate outliers occurring in the seams between images. Currently, Sentinel-1 data from GEE is already clamped to the 99th and 1st percentiles. All datasets, multispectral and SAR, were resampled to 20 m.

2.3. Classification

We based our classification scheme on the Millenium Assessment of Ecosystem Services (MAES), modified to include Ramsar wetland types (Fitoka et al., 2017), mapping the following ten classes: bare soil,

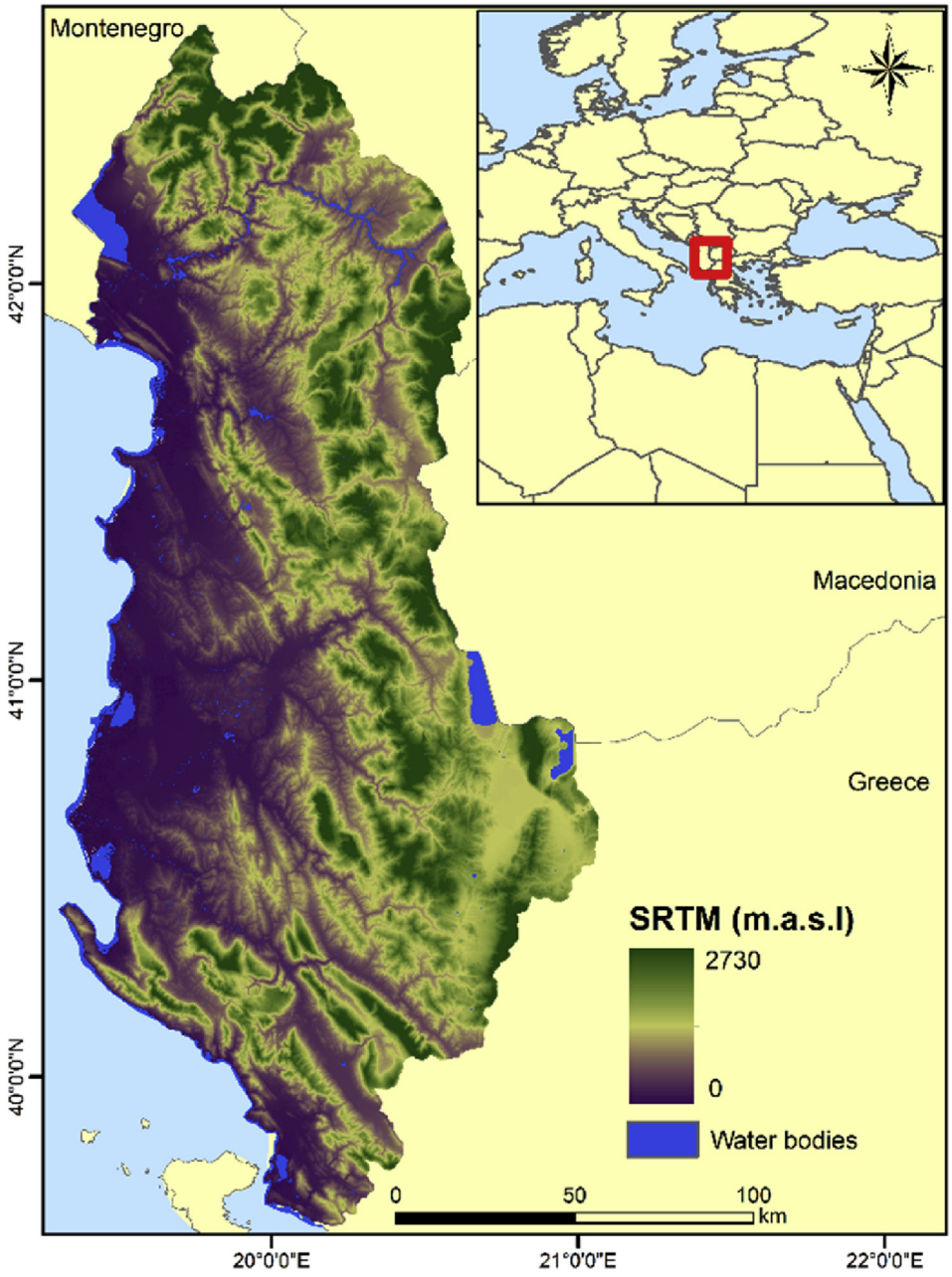

Figure 1. Location of Albania with its Digital Elevation Model and water bodies.

permanent water bodies, intermittent water bodies, marshlands, cropland, grassland, heathland and scrubland, deciduous forest, coniferous forest and built-up. "ntermittent water bodies" refer to areas that are bare when not inundated (e.g. intertidal mudflats and the water spread area of many water reservoirs). "Marshlands" are areas that have vegetation and water, at least temporarily. "Heathland and scrubland" are areas dominated by shrub-like vegetation. The other 7 classes are self-explanatory.

We applied a Random Forest (Breiman, 2001) classifier using 500 trees in GEE and collected a set of 300 polygons for training and validation. The polygons were delineated using aerial imagery of 2015 at 20 m and 8 m resolution, available at the portal of the State Authority for Geospatial Information (ASIG) (https://geoportal.asig.gov.al). Each class had circa 30 polygons about the same size except for the class "cropland" which were twice larger. This was necessary because it was the class with the largest extension and variability due to the different crops and rotation patterns. For each dataset and combination of datasets we performed a cross-validation in which 2/3 of the polygons within each class were randomly selected for training and 1/3 for validation.

2.4. Post-classification processing

The post-classification processing has two parts; removal of areas unlikely to be a wetland and prone to errors, and the application of knowledge-based rules.

The different datasets used have their own inherent noise and errors. For example, SAR data is prone to slant-range distortions (foreshortening and layover) in areas with a complex relief (White et al., 2015). Thus, we used morphological constrains to create a Potential Wetlands Mask (PWM) to mask out these artifacts that would cause classification errors. Out of the SRTM digital elevation model we calculated a set of 3 derivatives: Topographic Wetness Index (TWI) (Böhner J. and Selige T., 2006), Multiresolution Index of Valley Bottom Flatness (MrVBF) (Gallant

and Dowling, 2003), and the Terrain Surface Convexity Index (TSC) (Iwahashi and Pike, 2007). These datasets were combined with the Global Surface Water (GSW) product (Pekel et al., 2016) and then normalized to values from 0 to 1. The result is a map showing the likelihood of each pixel of being a wetland. We then divided this map into two categories: areas with potential for being a wetland (the PWM) and areas unlikely of being a wetland. In order to set the threshold between these two categories we used the Otsu histogram-based thresholding method (Otsu, 1979). This method maximizes interclass variance and it works best with bi-modal distributions, such as in our case. Training, classification and validation was limited to areas within the PWM. This way, artifacts produced by the terrain on SAR (slant-range) and in optical data (illumination angles) were reduced.

Statistical mapping (e.g. Random Forest) can seldom produce accurate results on its own. Knowledge-based criteria and ancillary information can be used to produce outputs with the thematic resolution and mapping accuracy needed (Connolly and Holden, 2009; Long and Skewes, 1996; Perennou et al., 2018; Van der Voorde et al., 2007). To that end, we applied an additional set of knowledge-based rules to further separate the land cover classes. These rules are based on theoretical considerations and observations, and are common practice to enhance the result of remote sensing-based classifications (Manandhar et al., 2009; Stefanov et al., 2001; Van der Voorde et al., 2007). To separate "riverbanks" from other bare surfaces we applied a 120 m buffer to the river network. All "heathland and scrubland" areas within this buffer were reclassified as "riverine scrubs". An additional class of "beaches and coastal dunes" was created for all bare surfaces within 50 m from the shoreline. Figure 2 shows the classification and post-classification workflow used. The final result is a classification of six wetlands classes (counting "beaches and coastal dunes" as a wetlands) and seven non-wetland classes.

2.5. Accuracy analysis

Besides the cross-validation applied to the results of the classification of each dataset (i.e. S1, S2, NDIs and their combinations) we performed an accuracy analysis of the final product (i.e. after the application of the post classification rules). For validating this dataset, we performed a stratified random sampling of 527 additional points using the platform Laco-wiki (See et al., 2017). The platform gives access to Google, Bing and satellite imagery enabling a visual interpretation of the validation samples and generates accuracy reports. Additionally, we compared our results with the last inventory of wetlands, carried out in 2001–2003 (Marieta et al., 2003). Through visual inspection we discarded from the inventory the wetlands that were not visible in current high resolution imagery and calculated the proportion of wetlands correctly identified.

3. Results

3.1. Impact of the different datasets on the mapping accuracy

This analysis was carried out with the 10 initial land cover classes and the results of the cross-validation; overall accuracy (OA), producers' accuracy (PA) and users' accuracy (UA). The classifications produced using the three datasets (S1, S2 and NDIs) or combining S1 and NDIs achieved the highest accuracies, followed by the combination of S1 and S2, and the combination of S2 and NDIs (Figure 3). When using each dataset separately, accuracies were significantly lower than any combination of multiple datasets.

When using S1 and NDIs for classification, the class "marshlands" occupied a larger area at the expense of "cropland" and "heathland and scrubland" (Table 1). When using S1 and S2, the class "intermittent water bodies" was overestimated at the expense of "permanent water", mostly at the sea. When using only the optical datasets (i.e. NDIs and S2) the class "built-up" was greatly overestimated at the expense of "bare soil" and "heathland and scrubland" (UA of built-up 69%, Appendix A).

Areas of steep slope oriented towards the Sentinel-1 satellite returned very high backscatter values, which misclassified as "Built-up" regardless of their true class. Despite the PWM excluded most of these errors, some remained along small rivers and creeks between steep mountains.

The distinction between "coniferous forest" and "deciduous forest" was equally good regardless of the combination of datasets used, as long as more than one were used. The confusion between "heathland and scrubland" and "grassland" was high for all combinations of datasets (e.g. UA of "heathland and scrubland" 52% and PA of "grasslands" 41% when using the three datasets, Appendix A).

The class "cropland" occupied the largest extent, and thus had a larger number of inconsistencies. For instance, some croplands were classified

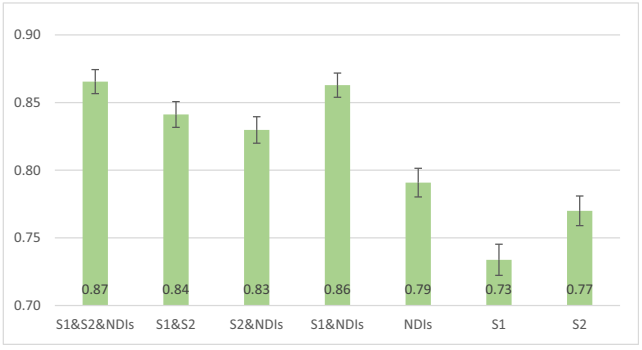

Figure 3. Overall accuracies of individual and combined datasets. Error bars indicate the standard deviation at 95% confidence interval.

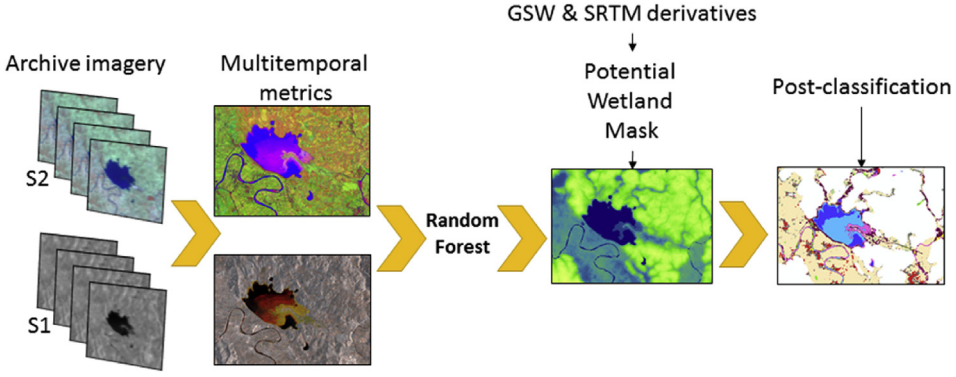

Figure 2. Classification workflow. S1 and S2 are the Sentinel-1 and Sentinel-2 image collections, out of which the different multitemporal metrics are calculated. During the post-classification phase we removed systematic errors using the PWM and added 3 new wetland classes using knowledge-based rules. The Potential Wetland Mask was generated out of the Global Surface Water (GSW) layer and SRTM digital elevation model derivatives.

Table 1. Number of hectares per class with each combination of multiple datasets before post-classification processing.

	S1&S2&NDI (ha)	S1 & S2 (ha)	S2 & NDI (ha)	S1 & NDI (ha)
Bare soil	15,749	18,642	7,714	15,104
Permanent Water	77,972	74,165	78,672	75,124
Built-up	30,782	30,440	54,033	32,955
Marshlands	30,803	22,848	25,732	41,794
Intermittent water	7,636	15,980	11,563	6999
Deciduous forest	32,144	33,859	30,388	30,364
Coniferous forest	12,771	17,674	13,879	13,858
Cropland	256,310	246,606	260,065	262,866
Grassland	28,378	26,792	35,259	27,426
Heathland and scrubland	105,883	111,420	81,121	91,935

as "heathland and scrubland" and others as "bare Soil". Many of them correspond to rather dry areas with high content in salt that are not actively farmed (Figure 4 A and B). Other croplands showed higher frequencies of inundation and were thus misclassified as "marshlands" (Figure 4 C and D). These were very localized cases easy to correct manually. The area shown in Figure 4 C and D actually corresponds to the former Maliqui freshwater marsh, recently drained and now used for agriculture.

3.2. Post-classification processing

Post-classification processing was applied only to the results of the combination of S1, S2 and NDIs datasets. Using knowledge-based criteria we incorporated three classes: "riverbanks", "riverine scrubs" and "dunes" increasing the wetland-related classes from 3 to 6 (Figure 5, and supplementary file Albania_PWA_LULC_2020.tif). This generated an inevitable trade-off between thematic resolution and classification accuracy, and some errors were introduced. For instance, a few bare soil areas of industrial use (e.g. ports or salt pans) were classified as "dunes" or "riverbanks".

The accuracy analysis with independent samples returned an overall accuracy of 82%. The detailed accuracy matrix (Appendix A) shows that most conflicting classes were "bare soil" and "riverine scrubs" that were often mixed up with "heathland and scrub". In addition, "heathland and scrub" was sometimes misclassified as "cropland", and "marshland" was sometimes confused with "intermittent water bodies".

Because the aim of this study is to apply the methodology at national scale, we compared our results with the last inventory of Albanian

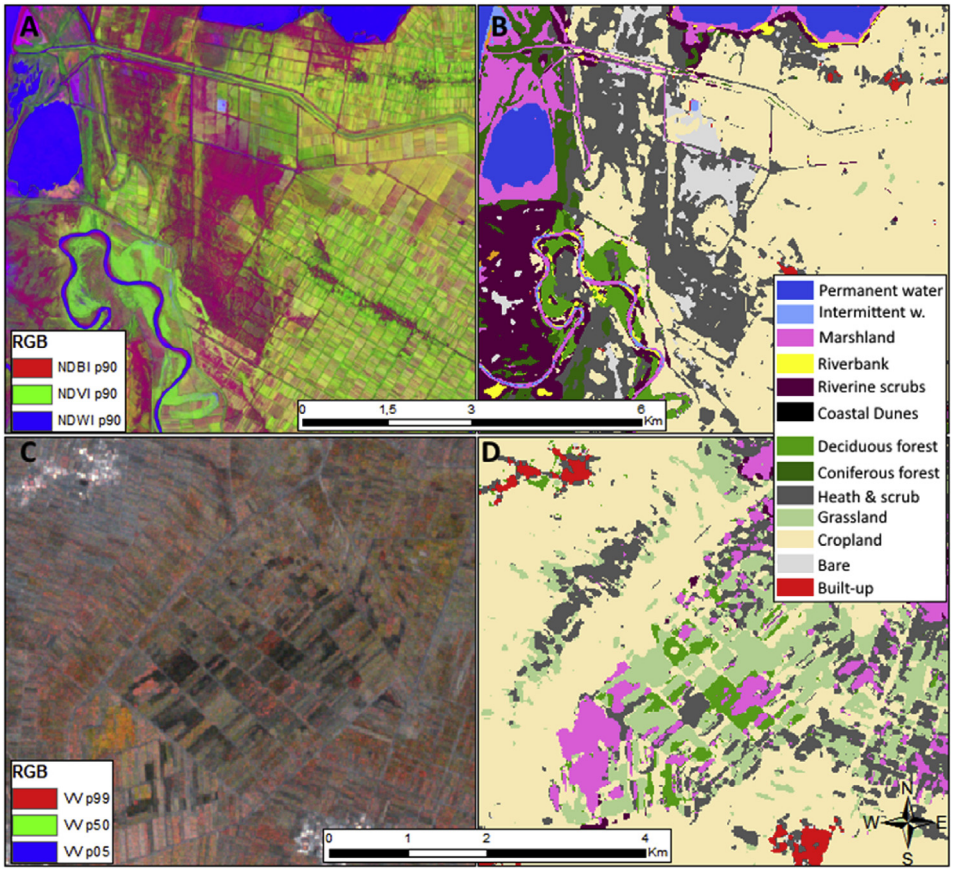

Figure 4. "Cropland" misclassified as "bare soil" and "heathland and scrub" (A and B) and as "marshlands" (C and D). "A" shows an RGB composite of NDBI, NDVI and NDWI. Red areas represent high NDBI values. "C" shows a Sentinel-1 RGB composite of percentiles 99, 50 and 05 of a former marshland, now used for agriculture. "B" and "D" show the classification results of "A" and "C" respectively.

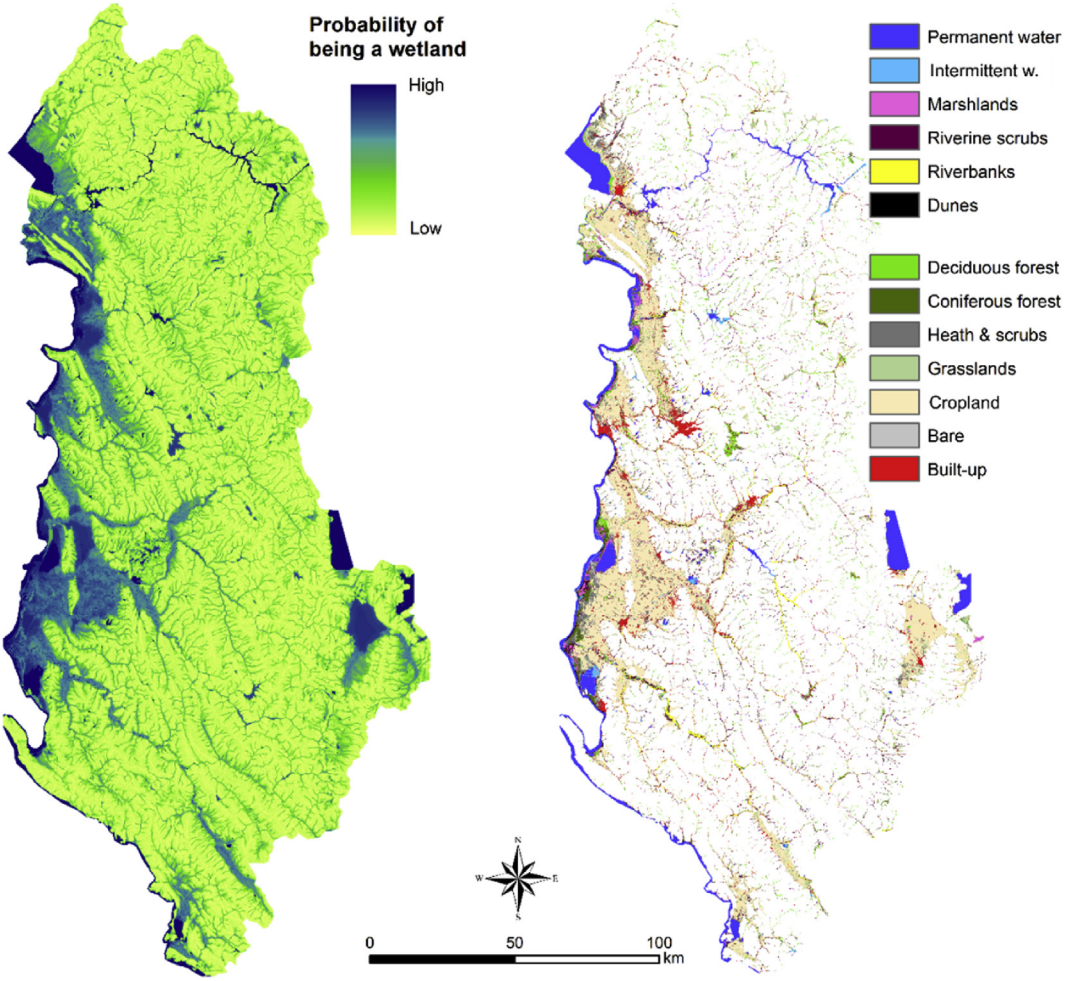

Figure 5. Map of potential wetlands (left) and map with the 13 final classes, result of the post-classification (right). The map of potential wetlands indicates the probability of each pixel of being a wetland according to morphological criteria. Only areas above a histogram-based threshold (Otsu, 1979) were mapped.

wetlands. It was carried out in 2003 using field information and satellite and aerial image interpretation (Marieta et al., 2003). Out of 694 inventoried wetlands, we eliminated 18 that we couldn't find through visual inspection of current imagery and are assumed to have disappeared. Fourteen of them were artificial water reservoirs, three marshes and one lake. For the remaining 676 wetlands we analyzed their correspondence with our results. The PWM excluded 99 wetlands. Thirty-three of those were small artificial water reservoirs, and 54 were very small glacial lakes (circa 1 ha). All the remaining 577 inventoried wetlands included within the PWM were classified as one of our 6 wetland classes.

4. Discussion

4.1. Impact of the different datasets on the mapping accuracy

Fusing the datasets from different sensors (Sentinel-1 and Sentinel-2) and the different indices (NDBI, NDVI, NDWI), provided the highest accuracies (Figure 3), in agreement with other studies (Blaes et al., 2005; Brisco and Brown, 1995; Chatziantoniou et al., 2017; Stefanski et al., 2014; Waske, 2014; White et al., 2017). SAR signals are sensitive to structure and biomass, dielectric properties of vegetation and soil (inundation patterns) and roughness (White et al., 2017, 2015). This makes SAR data essential to distinguish certain land cover classes such as "uilt-up" and "bare soil", or classes with different levels of moisture and inundation such as "intermittent water bodies" (Figure 6). Other studies using multitemporal metrics have reported high accuracies using only optical data (Inglada et al., 2017; Mack et al., 2017; Pflugmacher et al., 2019), but they only have one or two classes for wetlands, and therefore very high accuracies in their class "water". More recent studies reported high accuracies in wetlands when combining Sentinel-1 and 2 metrics, but only after excluding highly vegetated wetlands and for a relatively smaller area (Slagter et al., 2020).

Despite the fact that the NDIs were calculated from the same Sentinel-2 images, when combining both NDIs and S2 dataset, the accuracy increased significantly with respect to using only the S2 dataset. The NDIs dataset contains information on the temporal variation of physical and biological characteristics of the land cover (e.g. maximum inundation, vegetation peak, and minimum inundation and vegetation), while the S2 datasets contains only spectral information. The combination S2&NDIs even approached the performance accuracy levels of the combination S2&S1. This highlights on the importance of the temporal dimension when mapping dynamic cover types.

"Cropland" is also a very dynamic class due to management practices that are not constant across time nor space, making this class prone to errors. In our case, this caused a high rate of omission errors (i.e. "cropland" classified as something else, Figure 4 C and D). For instance, some croplands are harvested once, others twice (e.g. winter wheat) or not at all (i.e. fallow land and permanent crops), and other times are used for temporary grasslands, increasing the error rate (Mack et al., 2017; Stefanski et al., 2014). Systematic and standardized sampling campaigns such as the ones carried out at EU level within the LUCAS (Land Use-Cover Area frame Survey) project can be used to produce more accurate classifications including crop types (Mack et al., 2017; Pflugmacher et al., 2019). Unfortunately, such datasets are currently not

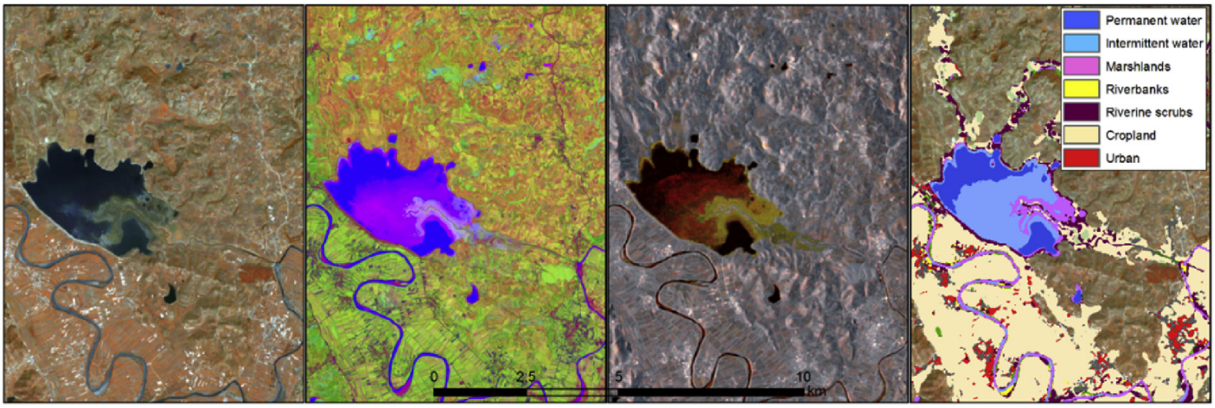

Figure 6. From left to right, an example of the datasets S2, NDIs, S1 and result of classification. NDIs and the S1 metrics allow to separate the parts of the wetland that are permanently and temporarily flooded.

available for Albania. It would be possible to use cadastral information to leave out areas used for agriculture and eliminate these uncertainties. However, many agricultural areas act as habitat for wetland species when the natural wetlands are dried out or disturbed, and should be included in wetland mapping activities (Czech and Parsons, 2002). Besides, for an integrated management that considers the water-food-and energy nexus it is important to include agricultural areas, whether they are in use or not (fallow).

Yearly water level fluctuations are common in artificial wetlands used as water reservoirs. These water bodies are often classified as one single class of permanent water, whereas they are composed of areas that are either permanently or temporarily inundated. The use of multitemporal statistics allowed us to separate these two categories (Figure 6). Mapping the intermittent water bodies is especially important in the case of water reservoirs. These areas are often steep and local mountainous vegetation cannot grow there due to the flood recurrence. This makes these areas prone to erosion, increasing the sediment deposition rate in the water reservoir and thus decreasing its life span. Mapping the water spread area (i.e. intermittent water) have been used before in sedimentation models to predict the life span of the dam (Foteh et al., 2018).

4.2. Post-classification processing

Often, land managers need higher accuracies and thematic resolutions, especially for quantitative analyses (Chatziantoniou et al., 2017; Manandhar et al., 2009). Using knowledge-based rules based on spatial, environmental, geomorphologic or ecological criteria can improve accuracies and the separability of classes that are spectrally similar but ecologically very different (Chatziantoniou et al., 2017; Manandhar et al., 2009). For instance, the mapping exercise of Pflugmacher et al. (2019) was carried out at continental scale. This implied mapping the same land cover types across climatic regions, where the same land cover type can display different spatiotemporal patterns (e.g. boreal coniferous forests vs. Mediterranean coniferous forests). To account for this, they implemented auxiliary variables that exploited the relationship between climate, topography and vegetation (precipitation, temperature, and latitude and longitude). The addition of these variables had the highest effect on model performance, higher even than adding other temporal metrics. Their results show the relevance of adding environmental information rather than just more remotely sensed data. The knowledge-based rules we set were proximity values based on theoretical considerations and observations. Their addition increased the thematic resolution, but also introduced some classification errors. This is something to be expected and good knowledge of the area is necessary to balance the trade-off between thematic resolution and classification accuracy (Knight et al., 2013). Knowledge-based rules require ecological rather than remote sensing expertise and are specific for each case study (Perennou et al., 2018). Thus, they should be modified according to the needs and conditions of other environments when replicating the methodology somewhere else. This, in turn, could pose an issue of lack of standardization. Regardless, our results provide supporting evidence of the benefits of including ancillary information based on logic and expert knowledge in mapping activities (Chatziantoniou et al., 2017; Long and Skewes, 1996; Manandhar et al., 2009), so that mapping products can be better suited for decision making. There is still a number of wetland classes that could not be included in this exercise due to lack of better training information (e.g. peatbogs).

The comparison of our final product with the 2003 inventory revealed that our workflow missed 99 of the 676 wetlands inventoried. Almost half of these were artificially created water reservoirs located in areas with a topography unsuitable to store water without building a dam, and therefore not regarded as potential wetland areas. However, there were 54 small glacial lakes (circa 1 ha) that were also masked out. Practically, all of these omission errors were initially classified as some wetland type before the PWM was applied. Omission errors can be avoided by applying a more conservative manual threshold to the PWM, but that can increase the number of errors related to the terrain artifacts. Trade-offs between omission and commission errors are often unavoidable and a histogram-based thresholding method is still recommended. Other types of wetlands such as raised peatbogs could be as well excluded when located on a slope.

5. Conclusions

The demanding monitoring and reporting requirements of the Ramsar Convention on Wetlands and the Sustainable Development Goals create a need for countries to improve their capabilities for wetland mapping, inventorying, monitoring and assessment. Landscape temporal dynamics are traits that have often hampered mapping activities, and in consequence delayed spatially-based decisions. Using a combination of multitemporal SAR and multispectral metrics we can use such traits to distinguish spectrally similar but ecologically different cover types. Including additional knowledge-based rules removes artifacts and increases the thematic resolution. Cloud computing platforms can facilitate the handling of large amounts of spatial data and allow to deliver ready to use products in an operational way.

Declarations

Author contribution statement

J. Muro: Conceived and designed the experiments; Performed the experiments; Analyzed and interpreted the data; Wrote the paper.

A. Varea: Performed the experiments.

A. Strauch: Conceived and designed the experiments; Contributed reagents, materials, analysis tools or data; Wrote the paper.

A. Guelmami: Conceived and designed the experiments; Performed the experiments; Analyzed and interpreted the data.

E. Fitoka: Contributed reagents, materials, analysis tools or data.

F. Thonfeld: Conceived and designed the experiments; Analyzed and interpreted the data.

B. Diekkrüger: Analyzed and interpreted the data; Wrote the paper.

B. Waske: Analyzed and interpreted the data; Contributed reagents, materials, analysis tools or data.

Funding statement

The SWOS project that provided the framework for the work presented here has received funding from the European Union's Horizon 2020 research and innovation program (Grant Agreement No. 348 642088).

Competing interest statement

The authors declare no conflict of interest.

Additional information

Supplementary content related to this article has been published online at https://doi.org/10.1016/j.heliyon.2020.e04496.

Acknowledgements

We are grateful to Gennadii Donchyts who developed and shared the cloud shadow mask for Sentinel-2.

Appendix A. Error matrix of the S1 & S2 & NDI classification after post-classification

	Bare Soil	Permanent water	Built-up	Marshlands	Intermitent water	Deciduous	Coniferous	Cropland	Grassland	Heath & scrub	Dunes	Riverbanks	Riverine scrubs	UA
Bare Soil	13	0	2	0	0	2	0	5	2	6	0	0	0	43%
Permanent water	0	76	0	1	0	0	0	0	0	0	0	0	0	99%
Built-up	0	0	19	0	0	3	0	2	0	4	0	2	0	63%
Marshland	0	0	0	16	6	4	2	0	1	0	0	1	0	53%
Intermittent water.	0	2	0	0	27	0	0	0	0	0	1	0	0	90%
Deciduous	0	0	0	0	0	30	0	1	0	1	0	0	0	94%
Coniferous	0	0	0	1	0	0	27	0	0	1	0	0	1	90%
Cropland	0	0	1	0	0	2	0	91	4	0	0	0	2	91%
Grassland	0	0	0	0	0	2	0	4	23	1	0	0	0	77%
Heath & scrub	1	0	3	0	0	1	0	16	1	22	0	0	0	50%
Dunes	2	1	0	0	0	0	1	1	0	0	25	0	0	83%
Riverbanks	1	0	0	0	1	1	0	0	0	1	0	26	0	87%
Riverine scrubs	0	0	4	0	0	3	0	4	2	5	0	2	14	41%
PA	59%	99%	66%	90%	55%	62%	88%	90%	56%	63%	83%	72%	71%	

References

Blaes, X., Vanhalle, L., Defourny, P., 2005. Efficiency of crop identification based on optical and SAR image time series. Remote Sens. Environ. 96, 352–365.

Böhner, J., Selige, T., 2006. Spatial prediction of soil attributes using terrain analysis and climate regionalisation. In: SAGA — Analysis and Modelling Applications. Verlag Erich Goltze GmbH, pp. 13–27.

Breiman, L., 2001. Random forests. Mach. Learn. 45, 5–32.

Brisco, B., Brown, R.J., 1995. Multidate SAR/TM synergism for crop classification in western Canada. Photogramm. Eng. Rem. Sens. 61, 1009–1014.

Carrasco, L., O'Neil, A., Morton, R., Rowland, C., 2019. Evaluating combinations of temporally aggregated sentinel-1, sentinel-2 and landsat 8 for land cover mapping with Google Earth engine. Rem. Sens. 11, 288.

Chatziantoniou, A., Psomiadis, E., Petropoulos, G., 2017. Co-orbital Sentinel 1 and 2 for LULC mapping with emphasis on wetlands in a mediterranean setting based on machine learning. Rem. Sens. 9, 1259.

Connolly, J., Holden, N.M., 2009. Mapping peat soils in Ireland: updating the derived Irish peat map. Ir. Geogr. 42, 343–352.

Czech, H.A., Parsons, K.C., 2002. Agricultural wetlands and waterbirds: a review. Waterbirds Int. J. Waterbird Biol. 25, 56–65.

Dixon, M.J.R., Loh, J., Davidson, N.C., Beltrame, C., Freeman, R., Walpole, M., 2016. Tracking global change in ecosystem area: the Wetland Extent Trends index. Biol. Conserv. 193, 27–35.

Dong, J., Xiao, X., Menarguez, M.A., Zhang, G., Qin, Y., Thau, D., Biradar, C., Moore, B., 2016. Mapping paddy rice planting area in northeastern Asia with Landsat 8 images, phenology-based algorithm and Google Earth Engine. Remote Sens. Environ. 185, 142–154.

EcoAlbania, 2017. Mapping of Hydropower Plant in Albania, Using GIS. EcoAlbania.

ESA, 2012. Sentinel-2: ESA's Optical High-Resolution Mission for GMES Operational Services (ESA SP-1322/2 March 2012).

FAO, 2015. FAO Country Programming Framework.

Finlayson, M., D'Cruz, R., Davidson, N., 2005. Ecosystems and human well-being: wetlands and water. Millenium Ecosystem Assessment. World Resources Institute.

Fitoka, E., Poulis, G., Perennou, C., Thulin, S., Abdul Malak, D., Franke, J., Guelmani, A., Schröeder, 2017. The Wetland Ecosystems in MAES Nomenclature.

Foteh, R., Garg, V., Nikam, B.R., Khadatare, M.Y., Aggarwal, S.P., Kumar, A.S., 2018. Reservoir sedimentation assessment through remote sensing and hydrological modelling. J. Indian Soc. Remote Sens. 46, 1893–1905.

Gallant, J.C., Dowling, T.I., 2003. A multiresolution index of valley bottom flatness for mapping depositional areas: multiresolution Valley Bottom flatness. Water Resour. Res. 39.

GEE, 2018. Sentinel-1 Algorithms in Google Earth Engine [WWW Document]. URL. https://developers.google.com/earth-engine/sentinel1.

Gevaert, C.M., García-Haro, F.J., 2015. A comparison of STARFM and an unmixing-based algorithm for Landsat and MODIS data fusion. Remote Sens. Environ. 156, 34–44.

Gorelick, N., Hancher, M., Dixon, M., Ilyushchenko, S., Thau, D., Moore, R., 2017. Google Earth engine: planetary-scale geospatial analysis for everyone. Remote Sens. Environ. 202, 18–27.

Griffiths, P., van der Linden, S., Kuemmerle, T., Hostert, P., 2013. A pixel-based landsat compositing algorithm for large area land cover mapping. IEEE J. Sel. Top. Appl. Earth Obs. Remote Sens. 6, 2088–2101.

Hardy, A., Ettritch, G., Cross, D., Bunting, P., Liywalii, F., Sakala, J., Silumesii, A., Singini, D., Smith, M., Willis, T., Thomas, C., 2019. Automatic detection of open and vegetated water bodies using Sentinel 1 to map african malaria vector mosquito breeding habitats. Rem. Sens. 11, 593.

Herold, M., Liu, X., Clarke, K.C., 2003. Spatial metrics and image texture for mapping urban land use. Photogramm. Eng. Rem. Sens. 69, 991–1001.

Hird, J., DeLancey, E., McDermid, G., Kariyeva, J., 2017. Google Earth engine, open-access satellite data, and machine learning in support of large-area probabilistic wetland mapping. Rem. Sens. 9, 1315.

Inglada, J., Vincent, A., Arias, M., Tardy, B., Morin, D., Rodes, I., 2017. Operational high resolution land cover map production at the country scale using satellite image time series. Rem. Sens. 9, 95.

Iwahashi, J., Pike, R.J., 2007. Automated classifications of topography from DEMs by an unsupervised nested-means algorithm and a three-part geometric signature. Geomorphology 86, 409–440.

Joshi, N., Baumann, M., Ehammer, A., Fensholt, R., Grogan, K., Hostert, P., Jepsen, M., Kuemmerle, T., Meyfroidt, P., Mitchard, E., Reiche, J., Ryan, C., Waske, B., 2016. A review of the application of optical and radar remote sensing data fusion to land use mapping and monitoring. Rem. Sens. 8, 70.

Knight, J.F., Tolcser, B.P., Corcoran, J.M., Rampi, L.P., 2013. The effects of data selection and thematic detail on the accuracy of high spatial resolution wetland classifications. Photogramm. Eng. Rem. Sens. 79, 613–623.

Lang, M., McCarty, G., Oesterling, R., Yeo, I.-Y., 2013. Topographic metrics for improved mapping of forested wetlands. Wetlands 33, 141–155.

Long, B.G., Skewes, T.D., 1996. A technique for mapping mangroves with landsat TM satellite data and geographic information system. Estuar. Coast Shelf Sci. 43, 373–381.

Mack, B., Leinenkugel, P., Kuenzer, C., Dech, S., 2017. A semi-automated approach for the generation of a new land use and land cover product for Germany based on Landsat time-series and Lucas *in-situ* data. Remote Sens. Lett. 8, 244–253.

Mahdianpari, M., Salehi, B., Mohammadimanesh, F., Homayouni, S., Gill, E., 2018. The first wetland inventory map of newfoundland at a spatial resolution of 10 m using sentinel-1 and sentinel-2 data on the Google Earth engine cloud computing platform. Rem. Sens. 11, 43.

Manandhar, R., Odeh, I., Ancev, T., 2009. Improving the accuracy of land use and land cover classification of landsat data using post-classification enhancement. Rem. Sens. 1, 330–344.

Marieta, M., Fitoka, E., Bego, F., 2003. Inventory of Albanian Wetlands. ECAT and Greek Biotope/Wetland Centre (EKBY). Thermi, Greece.

Mc Feeters, S.K., 1996. The use of the Normalized Difference Water Index (NDWI) in the delineation of open water features. Int. J. Rem. Sens. 17, 1425–1432.

Mitsch, W.J., Gosselink, J.G., 2000. The value of wetlands: importance of scale and landscape setting. Ecol. Econ. 35, 25–33.

Muro, J., Strauch, A., Fitoka, E., Tompoulidou, M., Thonfeld, F., 2019. Mapping wetland dynamics with SAR-based change detection in the cloud. Geosci. Rem. Sens. Lett. IEEE 1–4.

Otsu, N., 1979. A threshold selection method from gray-level histograms. IEEE Trans. Syst. Man Cybern. 9, 62–66.

Paganini, M., Petiteville, I., Ward, S., Dyke, G., Steventon, M., Harry, J., Kerblat, F., 2018. Satellite Earth Observations in Support of the Sustainable Development Goals. ESA.

Patel, N.N., Angiuli, E., Gamba, P., Gaughan, A., Lisini, G., Stevens, F.R., Tatem, A.J., Trianni, G., 2015. Multitemporal settlement and population mapping from landsat using Google Earth engine. Int. J. Appl. Earth Obs. Geoinformation 35, 199–208.

Pekel, J.-F., Cottam, A., Gorelick, N., Belward, A.S., 2016. High-resolution mapping of global surface water and its long-term changes. Nature 540, 418–422.

Perennou, C., Guelmami, A., Paganini, M., Philipson, P., Poulin, B., Strauch, A., Tottrup, C., Truckenbrodt, J., Geijzendorffer, I.R., 2018. Mapping mediterranean wetlands with remote sensing: a good-looking map is not always a good map. In: Advances in Ecological Research. Elsevier, pp. 243–277.

Perennou, C., Machado Beltrame, C., Guelmani, A., Vives, T., Caessteker, P.T., 2012. Existing areas and past changes of wetland extent in the Mediterranean region: an overview. Ecol. Mediterr. 38 (2).

Pflugmacher, D., Rabe, A., Peters, M., Hostert, P., 2019. Mapping pan-European land cover using Landsat spectral-temporal metrics and the European LUCAS survey. Remote Sens. Environ. 221, 583–595.

Ramsar Convention on Wetlands, 2018. Global Wetland Outlook: State of the World's Wetlands and Their Services to People. Ramsar Convention Secretariat, Gland, Switzerland.

Russi, D., ten Brink, P., Farmer, A., Badura, T., Coates, D., Förster, J., Kumar, R., Davidson, N., 2012. The Economics of Ecosystems and Biodiversity for Water and Wetlands (Final Consultation Draft), A Contribution to CBD COP2011. Ramsar.

See, L., Laso Bayas, J., Schepaschenko, D., Perger, C., Dresel, C., Maus, V., Salk, C., Weichselbaum, J., Lesiv, M., McCallum, I., Moorthy, I., Fritz, S., 2017. LACO-wiki: a new online land cover validation tool demonstrated using GlobeLand30 for Kenya. Rem. Sens. 9, 754.

Sikorova, K., Gallop, P., 2015. Financing for Hydropower in Protected Areas in Southeast Europe. CEE Nankwatch Network.

Slagter, B., Tsendbazar, N.-E., Vollrath, A., Reiche, J., 2020. Mapping wetland characteristics using temporally dense Sentinel-1 and Sentinel-2 data: a case study in the St. Lucia wetlands, South Africa. Int. J. Appl. Earth Obs. Geoinformation 86, 102009.

Stefanov, W.L., Ramsey, M.S., Christensen, P.R., 2001. Monitoring urban land cover change. Remote Sens. Environ. 77, 173–185.

Stefanski, J., Kuemmerle, T., Chaskovskyy, O., Griffiths, P., Havryluk, V., Knorn, J., Korol, N., Sieber, A., Waske, B., 2014. Mapping land management regimes in western Ukraine using optical and SAR data. Rem. Sens. 6, 5279–5305.

Tucker, C.J., 1979. Red and photographic infrared linear combinations for monitoring vegetation. Remote Sens. Environ. 8, 127–150.

UN Stats Metadata Repository [WWW Document], 2018. URL. https://unstats.un.org/sdgs/metadata.

Van der Voorde, T., De Genst, W., Canters, F., 2007. Pixel-based VHR land-cover classifications of urban areas with post-classification techniques. Photogramm. Eng. Rem. Sens. 73, 1017–1027.

Vejnovic, I., Gallop, P., 2018. Financing for Hydropower in Protected Areas in Southeast Europe: 2018 Update. CEE Nankwatch Network.

Waske, B., 2014. Synergies from SAR-optical data fusion for LULC mapping. In: Manakos, I., Braun, M. (Eds.), Land use and land cover mapping in Europe. Springer Netherlands, Dordrecht, pp. 179–191.

Waske, B., Benediktsson, J.A., 2007. Fusion of support vector machines for classification of multisensor data. IEEE Trans. Geosci. Rem. Sens. 45, 3858–3866.

Weiss, S., Apostolau, A., Dug, S., Marcic, Z., Musovic, M., Oikonomou, A., Shumka, S., Skrijelj, R., Simonovic, P., Vesnic, A., Zabric, D., 2018. Endangered Fish Species in Balkan Rivers: their distributions and threats from hydropower development. Riverwatch & EuroNatur.

White, L., Brisco, B., Dabboor, M., Schmitt, A., Pratt, A., 2015. A collection of SAR methodologies for monitoring wetlands. Rem. Sens. 7, 7615–7645.

White, L., Millard, K., Banks, S., Richardson, M., Pasher, J., Duffe, J., 2017. Moving to the RADARSAT constellation mission: comparing synthesized compact polarimetry and dual polarimetry data with fully polarimetric RADARSAT-2 data for image classification of peatlands. Rem. Sens. 9, 573.

Wilkinson, G.G., 1996. A review of current issues in the integration of GIS and remote sensing data. Int. J. Geogr. Inf. Syst. 10, 85–101.

Xiong, J., Thenkabail, P., Tilton, J., Gumma, M., Teluguntla, P., Oliphant, A., Congalton, R., Yadav, K., Gorelick, N., 2017. Nominal 30-m cropland extent map of continental africa by integrating pixel-based and object-based algorithms using sentinel-2 and landsat-8 data on Google Earth engine. Rem. Sens. 9, 1065.

Zha, Y., Gao, J., Ni, S., 2003. Use of normalized difference built-up index in automatically mapping urban areas from TM imagery. Int. J. Rem. Sens. 24, 583–594.

Zhu, Z., Woodcock, C.E., 2014. Continuous change detection and classification of land cover using all available Landsat data. Remote Sens. Environ. 144, 152–171.